Materials Transactions, Vol. 49, No. 11 (2008) pp. 2534 to 2540
Special Issue on Advances in Computational Materials Science and Engineering V

Thermodynamic Analysis of the Phase Equilibria in the Fe-Zr-B System

Tatsuya Tokunaga[1,*1], Ken Terashima[2,*2], Hiroshi Ohtani[3] and Mitsuhiro Hasebe[3]

[1]*Department of Applied Science for Integrated System Engineering, Kyushu Institute of Technology, Kitakyushu 804-8550, Japan*
[2]*Graduate School, Kyushu Institute of Technology, Kitakyushu 804-8550, Japan*
[3]*Department of Materials Science and Engineering, Kyushu Institute of Technology, Kitakyushu 804-8550, Japan*

A thermodynamic analysis of the Fe-Zr-B ternary system has been carried out using the CALPHAD method. Among the three binary systems present in the ternary phase diagram, the thermodynamic descriptions of the Fe-Zr and Fe-B binary systems were taken from reported results and from our previous study, respectively. The thermodynamic parameters of the Zr-B binary system were evaluated using the thermochemical properties from our first-principles calculations, as well as available experimental data. In this modelling, the Gibbs energy of ZrB_2 with an AlB_2-type structure was represented using the two-sublattice model, in which vacancies were introduced into both the Zr and the B sublattices, following the recent data obtained from neutron diffraction experiments on NbB_2 with the same structure as that of ZrB_2. The optimized thermodynamic parameters of the Zr-B system enabled us to obtain reproducible calculations of the experimental data on phase boundaries and formation enthalpies obtained from first-principles calculations. The ternary parameters were determined using the experimental data on phase boundaries. The calculated results have nicely reproduced the experimental Fe-Zr-B ternary phase diagrams.
[doi:10.2320/matertrans.MB200809]

(Received May 1, 2008; Accepted August 13, 2008; Published October 3, 2008)

Keywords: *thermodynamic analysis, phase equilibria, calculation of phase diagrams (CALPHAD), first-principles calculations*

1. Introduction

It is well known that Fe-M-B amorphous alloys (where M = Zr, Hf, and Nb) exhibit excellent soft magnetic properties on crystallization.[1–4] The crystallized microstructure consists of a large portion of αFe grains embedded in a small fraction of the residual amorphous phase. As the nanocrystalline structure is formed in the primary crystallization reaction from the amorphous phase, much attention has been paid to the mechanism of the nanocrystalline structural evolution in these alloys.[5] Furthermore, to improve their soft magnetic properties and their glass-forming ability, the effect of the addition of a small amount of alloying elements has also been investigated.

The Fe-Zr-B ternary system is one of the basic constituent systems relevant to Fe-based magnetic materials. Therefore, it is useful to obtain knowledge on the phase equilibria in this ternary system to provide basic information for understanding of the crystallization behaviour and for further development of these soft magnetic materials.

In this study, to elucidate the phase equilibria in the Fe-Zr-B ternary system, we initially evaluated the thermodynamic properties of various borides appearing in the Zr-B binary system based on first-principles calculations, and then a thermodynamic analysis of the Fe-Zr-B ternary system was carried out using the CALPHAD method, by combining the formation enthalpies obtained from first-principles calculations with the reported experimental data.

2. Calculation Procedures

2.1 First-principles calculations

The energy of formation of Zr-based binary borides was calculated using the WIEN2k software package,[6] based on the Full Potential Linearized Augmented Plane Wave (FLAPW) method with a General Gradient Approximation (GGA).[7] Muffin-tin radii of 2.0 au (0.106 nm) for Zr and 1.4 au (0.074 nm) for B were assumed, and the plane wave basis set up to the cut-off energy of 20 Ry (270 eV) was utilized. The calculation of the total energy for each boride was based on the structural data compiled by Villars,[8] which provides information on the atomic positions for various borides.

Then, the energy of formation of the boride Zr_mB_n per mole of atoms, $\Delta E_{\text{form}}^{Zr_mB_n}$, was obtained as:

$$\Delta E_{\text{form}}^{Zr_mB_n} = E_{\text{total}}^{Zr_mB_n} - \frac{m}{m+n} E_{\text{total}}^{\text{hcp-Zr}} - \frac{n}{m+n} E_{\text{total}}^{\text{rhombohedral-}\alpha\text{B}} \quad (1)$$

where the terms $E_{\text{total}}^{Zr_mB_n}$, $E_{\text{total}}^{\text{hcp-Zr}}$, and $E_{\text{total}}^{\text{rhombohedral-}\alpha\text{B}}$ denote the total energy of the boride Zr_mB_n, hcp Zr, and rhombohedral αB, respectively.

2.2 Thermodynamic modelling

A description of the Gibbs energy for each phase appearing in the Fe-Zr-B ternary system will be presented in this section.

The regular solution approximation was applied to the liquid and primary solid solution phases. The molar Gibbs energy of the ϕ phase was described using the following equation:

$$\begin{aligned} G_{\text{m}}^{\phi} = {} & x_{\text{B}}{}^{\circ}G_{\text{B}}^{\phi} + x_{\text{Fe}}{}^{\circ}G_{\text{Fe}}^{\phi} + x_{\text{Zr}}{}^{\circ}G_{\text{Zr}}^{\phi} \\ & + RT(x_{\text{B}} \ln x_{\text{B}} + x_{\text{Fe}} \ln x_{\text{Fe}} + x_{\text{Zr}} \ln x_{\text{Zr}}) \\ & + x_{\text{B}}x_{\text{Fe}}L_{\text{B,Fe}}^{\phi} + x_{\text{B}}x_{\text{Zr}}L_{\text{B,Zr}}^{\phi} + x_{\text{Fe}}x_{\text{Zr}}L_{\text{Fe,Zr}}^{\phi} \\ & + x_{\text{B}}x_{\text{Fe}}x_{\text{Zr}}L_{\text{B,Fe,Zr}}^{\phi} \end{aligned} \quad (2)$$

where x_i denotes the mole fraction of element i, R is the universal gas constant, and T is temperature in Kelvin. The term ${}^{\circ}G_i^{\phi}$ denotes the Gibbs energy of element i in the ϕ phase and is called the lattice stability parameter. The descriptions of the lattice stability parameters for each pure element were

*1Corresponding author, E-mail: ttokunag@tobata.isc.kyutech.ac.jp
*2Graduate Student, Kyushu Institute of Technology

taken from the Scientific Group Thermodata Europe (SGTE) data.[9] The parameter $L^{\phi}_{i,j}$ denotes the interaction energy between i and j in the ϕ phase and has a compositional dependency using an n-th degree Redlich-Kister polynomial[10] as follows:

$$L^{\phi}_{i,j} = {}^0L^{\phi}_{i,j} + {}^1L^{\phi}_{i,j}(x_i - x_j) + {}^2L^{\phi}_{i,j}(x_i - x_j)^2 + \cdots + {}^nL^{\phi}_{i,j}(x_i - x_j)^n \quad (3)$$

where:

$${}^nL^{\phi}_{i,j} = a_n + b_nT. \quad (4)$$

The term $L^{\phi}_{\mathrm{B,Fe,Zr}}$ is the ternary interaction parameter between B, Fe, and Zr. The compositional dependency of this parameter is expressed as follows:

$$L^{\phi}_{\mathrm{B,Fe,Zr}} = x_{\mathrm{B}}{}^0L^{\phi}_{\mathrm{B,Fe,Zr}} + x_{\mathrm{Fe}}{}^1L^{\phi}_{\mathrm{B,Fe,Zr}} + x_{\mathrm{Zr}}{}^2L^{\phi}_{\mathrm{B,Fe,Zr}}. \quad (5)$$

It should be noted that boron was treated as a substitutional species in both bcc and fcc Fe in this modelling, following recent results by our group.[11] In that study, a ground state analysis using first-principles calculations showed that various bcc- and fcc-based Fe-B binary superstructures with boron occupying substitutional sites were more energetically stable than those with boron occupying octahedral interstitial sites in the ground state.

The contribution to the Gibbs energy from ferromagnetic ordering was taken into account in the bcc Fe and fcc Fe solid solution phases.[12,13]

Regarding the compound phase with some degree of homogeneity range, the Gibbs energy was represented using the sublattice model.[14]

For the Fe-Zr binary compound phases, Fe_2Zr, $FeZr_2$, and $FeZr_3$, the formulae $(Fe,Zr)_2(Fe,Zr)_1$, $(Fe,Zr)_1(Fe,Zr)_2$, and $(Fe,Zr)_1(Fe,Zr)_3$, were used, respectively. For the case of the phase with the formula $(Fe,Zr)_m(Fe,Zr)_n$, where m and n are the numbers of the sites of Sublattice 1 and Sublattice 2, respectively, the Gibbs energy of this phase per mole of formula unit was described using the following equation:

$$\begin{aligned} G^{\mathrm{Fe}_m\mathrm{Zr}_n}_{\mathrm{m}} = {} & y^{(1)}_{\mathrm{Fe}}(y^{(2)}_{\mathrm{Fe}}{}^{\circ}G^{\mathrm{Fe}_m\mathrm{Zr}_n}_{\mathrm{Fe:Fe}} + y^{(2)}_{\mathrm{Zr}}{}^{\circ}G^{\mathrm{Fe}_m\mathrm{Zr}_n}_{\mathrm{Fe:Zr}}) \\ & + y^{(1)}_{\mathrm{Zr}}(y^{(2)}_{\mathrm{Fe}}{}^{\circ}G^{\mathrm{Fe}_m\mathrm{Zr}_n}_{\mathrm{Zr:Fe}} + y^{(2)}_{\mathrm{Zr}}{}^{\circ}G^{\mathrm{Fe}_m\mathrm{Zr}_n}_{\mathrm{Zr:Zr}}) \\ & + mRT(y^{(1)}_{\mathrm{Fe}}\ln y^{(1)}_{\mathrm{Fe}} + y^{(1)}_{\mathrm{Zr}}\ln y^{(1)}_{\mathrm{Zr}}) \\ & + nRT(y^{(2)}_{\mathrm{Fe}}\ln y^{(2)}_{\mathrm{Fe}} + y^{(2)}_{\mathrm{Zr}}\ln y^{(2)}_{\mathrm{Zr}}) + {}^{\mathrm{ex}}G^{\mathrm{Fe}_m\mathrm{Zr}_n}. \end{aligned} \quad (6)$$

The term y^s_i denotes the site fraction of element i on the s-th sublattice, and ${}^{\circ}G^{\mathrm{Fe}_m\mathrm{Zr}_n}_{i:j}$ denotes the Gibbs energy of a hypothetical compound, i_mj_n, in which all the sites in Sublattice 1 are occupied by element i, and all the sites in Sublattice 2 are occupied by element j. The term ${}^{\mathrm{ex}}G^{\mathrm{Fe}_m\mathrm{Zr}_n}$ is the excess Gibbs energy term containing the interaction energy between unlike atoms, and is expressed by the following equation:

$$\begin{aligned} {}^{\mathrm{ex}}G^{\mathrm{Fe}_m\mathrm{Zr}_n} = {} & y^{(1)}_{\mathrm{Fe}}y^{(1)}_{\mathrm{Zr}}(y^{(2)}_{\mathrm{Fe}}L^{\mathrm{Fe}_m\mathrm{Zr}_n}_{\mathrm{Fe,Zr:Fe}} + y^{(2)}_{\mathrm{Zr}}L^{\mathrm{Fe}_m\mathrm{Zr}_n}_{\mathrm{Fe,Zr:Zr}}) \\ & + y^{(2)}_{\mathrm{Fe}}y^{(2)}_{\mathrm{Zr}}(y^{(1)}_{\mathrm{Fe}}L^{\mathrm{Fe}_m\mathrm{Zr}_n}_{\mathrm{Fe:Fe,Zr}} + y^{(1)}_{\mathrm{Zr}}L^{\mathrm{Fe}_m\mathrm{Zr}_n}_{\mathrm{Zr:Fe,Zr}}) \end{aligned} \quad (7)$$

where $L^{\mathrm{Fe}_m\mathrm{Zr}_n}_{i,j:k}$ (or $L^{\mathrm{Fe}_m\mathrm{Zr}_n}_{i:j,k}$) is the interaction parameter between unlike atoms on the same sublattice, and its compositional dependency is described using an equation similar to eq. (3).

For the ZrB_2 phase, we adopted the formula $(Va,Zr)_1(B,Va)_2$, where Va denotes a vacancy, based on recent data obtained from neutron diffraction experiments on NbB_2 with the same structure as that of ZrB_2,[15] where a vacancy was introduced in the Zr sites to account for its hyper-stoichiometric composition. The Gibbs energy of this phase per mole of formula unit is given by:

$$\begin{aligned} G^{\mathrm{ZrB_2}}_{\mathrm{m}} = {} & y^{(1)}_{\mathrm{Va}}(y^{(2)}_{\mathrm{B}}{}^{\circ}G^{\mathrm{ZrB_2}}_{\mathrm{Va:B}} + y^{(2)}_{\mathrm{Va}}{}^{\circ}G^{\mathrm{ZrB_2}}_{\mathrm{Va:Va}}) \\ & + y^{(1)}_{\mathrm{Zr}}(y^{(2)}_{\mathrm{B}}{}^{\circ}G^{\mathrm{ZrB_2}}_{\mathrm{Zr:B}} + y^{(2)}_{\mathrm{Va}}{}^{\circ}G^{\mathrm{ZrB_2}}_{\mathrm{Zr:Va}}) \\ & + RT(y^{(1)}_{\mathrm{Va}}\ln y^{(1)}_{\mathrm{Va}} + y^{(1)}_{\mathrm{Zr}}\ln y^{(1)}_{\mathrm{Zr}}) \\ & + 2RT(y^{(2)}_{\mathrm{B}}\ln y^{(2)}_{\mathrm{B}} + y^{(2)}_{\mathrm{Va}}\ln y^{(2)}_{\mathrm{Va}}) \\ & + y^{(1)}_{\mathrm{Va}}y^{(1)}_{\mathrm{Zr}}(y^{(2)}_{\mathrm{B}}L^{\mathrm{ZrB_2}}_{\mathrm{Va,Zr:B}} + y^{(2)}_{\mathrm{Va}}L^{\mathrm{ZrB_2}}_{\mathrm{Va,Zr:Va}}) \\ & + y^{(2)}_{\mathrm{B}}y^{(2)}_{\mathrm{Va}}(y^{(1)}_{\mathrm{Va}}L^{\mathrm{ZrB_2}}_{\mathrm{Va:B,Va}} + y^{(1)}_{\mathrm{Zr}}L^{\mathrm{ZrB_2}}_{\mathrm{Zr:B,Va}}). \end{aligned} \quad (8)$$

The meanings of the terms appearing in eq. (8) are the same as those in eqs. (6) and (7).

The remaining compound phases were treated as being stoichiometric compounds. For example, the Gibbs energy of the Fe_2B phase per mole of formula unit was described as follows:

$$G^{\mathrm{Fe_2B}}_{\mathrm{Fe:B}} - 2{}^{\circ}G^{\alpha\mathrm{Fe}}_{\mathrm{Fe}} - {}^{\circ}G^{\beta\mathrm{B}}_{\mathrm{B}} = a + bT \quad (9)$$

where the terms a and b correspond to the enthalpy and entropy terms to be evaluated in the thermodynamic analysis, respectively. As will be described in Section 3.2, the Gibbs energy of all the borides was represented relative to βB rather than to αB.

3. Results and Discussion

3.1 The Fe-Zr binary system

The Fe-Zr binary system is composed of a liquid (L), bcc ((αFe), (δFe), and (βZr)), fcc ((γFe)), hcp ((αZr)), and four intermetallic compounds, $Fe_{23}Zr_6$, Fe_2Zr, $FeZr_2$, and $FeZr_3$.[16] The Fe-Zr phase diagram has been updated recently,[17] including new experimental results,[18] where βFe_2Zr was found to exist rather than $Fe_{23}Zr_6$. However, for this binary system, the thermodynamic parameters assessed by Jiang *et al.*,[19] based on Ref. 16), were adopted in this study and are listed in Table 1. The calculated Fe-Zr binary phase diagram is shown in Fig. 1.

3.2 The Fe-B binary system

The equilibrium phases in the Fe-B binary system are: a liquid (L), bcc ((αFe), (δFe)), fcc ((γFe)), rhombohedral ((βB)), Fe_2B, and FeB.[20] Thermodynamic analyses have been performed by several researchers,[20–27] assuming a substitutional solid solution and/or an interstitial solid solution of boron. More recently, our group has carried out a thermodynamic assessment by combining the first-principles and CALPHAD methods.[11] In this study, the thermodynamic parameters assessed by our group, which reproduced first-principles results as well as available experimental data, were adopted and are listed in Table 1. The calculated Fe-B binary phase diagram is shown in Fig. 2.

3.3 The Zr-B binary system

The Zr-B binary phase diagram has been proposed by Okamoto[28] based on available literature data,[29–36] as shown in Fig. 3(a), where we made a slight modification to the allotropic transformation temperature of Zr. The given phase

Table 1 The evaluated thermodynamic parameters of the Fe-Zr-B ternary system.

System	Phase	Thermodynamic parameters, J/mol	Reference
Fe-Zr	L	${}^{0}L^{\mathrm{L}}_{\mathrm{Fe,Zr}} = -87715.0889 + 18.6901738\ T$	19)
		${}^{1}L^{\mathrm{L}}_{\mathrm{Fe,Zr}} = -20078.7306 + 16.2699408\ T$	
		${}^{2}L^{\mathrm{L}}_{\mathrm{Fe,Zr}} = -13743.1409$	
	(αFe)	${}^{0}L^{(\alpha\mathrm{Fe})}_{\mathrm{Fe,Zr}} = -42806.5566 + 14.0909459\ T$	
	((δFe), (βZr))	${}^{1}L^{(\alpha\mathrm{Fe})}_{\mathrm{Fe,Zr}} = -8247.63201$	
	(αZr)	${}^{0}L^{(\alpha\mathrm{Zr})}_{\mathrm{Fe,Zr}} = -10000 + 10T$	
		${}^{1}L^{(\alpha\mathrm{Zr})}_{\mathrm{Fe,Zr}} = -25297.5251$	
	(γFe)	${}^{0}L^{(\gamma\mathrm{Fe})}_{\mathrm{Fe,Zr}} = -48765.9442 + 9.29324141\ T$	
	$Fe_{23}Zr_6$	${}^{\circ}G^{\mathrm{Fe_{23}Zr_6}}_{\mathrm{Fe:Zr}} - 23{}^{\circ}G^{\alpha\mathrm{Fe}}_{\mathrm{Fe}} - 6{}^{\circ}G^{\alpha\mathrm{Zr}}_{\mathrm{Zr}} = -694724 + 3387.8902\ T$	
	Fe_2Zr	${}^{\circ}G^{\mathrm{Fe_2Zr}}_{\mathrm{Fe:Fe}} - 3{}^{\circ}G^{\alpha\mathrm{Fe}}_{\mathrm{Fe}} = +15000$	
		${}^{\circ}G^{\mathrm{Fe_2Zr}}_{\mathrm{Zr:Fe}} - 2{}^{\circ}G^{\alpha\mathrm{Fe}}_{\mathrm{Fe}} - {}^{\circ}G^{\alpha\mathrm{Zr}}_{\mathrm{Zr}} = +15000$	
		${}^{\circ}G^{\mathrm{Fe_2Zr}}_{\mathrm{Fe:Zr}} - 2{}^{\circ}G^{\alpha\mathrm{Fe}}_{\mathrm{Fe}} - {}^{\circ}G^{\alpha\mathrm{Zr}}_{\mathrm{Zr}} = -96914.1 + 350.4714\ T - 65.7354\ T\ln T - 0.01545\ T^2$	
		${}^{\circ}G^{\mathrm{Fe_2Zr}}_{\mathrm{Zr:Zr}} - 3{}^{\circ}G^{\alpha\mathrm{Zr}}_{\mathrm{Zr}} = +15000$	
		${}^{0}L^{\mathrm{Fe_2Zr}}_{\mathrm{Fe,Zr:Fe}} = +50000$	
		${}^{0}L^{\mathrm{Fe_2Zr}}_{\mathrm{Fe,Zr:Zr}} = +50000$	
		${}^{0}L^{\mathrm{Fe_2Zr}}_{\mathrm{Fe:Fe,Zr}} = -3305.01061$	
		${}^{0}L^{\mathrm{Fe_2Zr}}_{\mathrm{Zr:Fe,Zr}} = -3305.01061$	
	$FeZr_2$	${}^{\circ}G^{\mathrm{FeZr_2}}_{\mathrm{Fe:Fe}} - 3{}^{\circ}G^{\alpha\mathrm{Fe}}_{\mathrm{Fe}} = +15000$	
		${}^{\circ}G^{\mathrm{FeZr_2}}_{\mathrm{Zr:Fe}} - 2{}^{\circ}G^{\alpha\mathrm{Fe}}_{\mathrm{Fe}} - {}^{\circ}G^{\alpha\mathrm{Zr}}_{\mathrm{Zr}} = +15000$	
		${}^{\circ}G^{\mathrm{FeZr_2}}_{\mathrm{Fe:Zr}} - {}^{\circ}G^{\alpha\mathrm{Fe}}_{\mathrm{Fe}} - 2{}^{\circ}G^{\alpha\mathrm{Zr}}_{\mathrm{Zr}} = -70457.65071 + 19.8877704\ T$	
		${}^{\circ}G^{\mathrm{FeZr_2}}_{\mathrm{Zr:Zr}} - 3{}^{\circ}G^{\alpha\mathrm{Zr}}_{\mathrm{Zr}} = +15000$	
		${}^{0}L^{\mathrm{FeZr_2}}_{\mathrm{Fe,Zr:Fe}} = +8000$	
		${}^{0}L^{\mathrm{FeZr_2}}_{\mathrm{Fe,Zr:Zr}} = +8000$	
		${}^{0}L^{\mathrm{FeZr_2}}_{\mathrm{Fe:Fe,Zr}} = +80000$	
		${}^{0}L^{\mathrm{FeZr_2}}_{\mathrm{Zr:Fe,Zr}} = +80000$	
	$FeZr_3$	${}^{\circ}G^{\mathrm{FeZr_3}}_{\mathrm{Fe:Fe}} - 4{}^{\circ}G^{\alpha\mathrm{Fe}}_{\mathrm{Fe}} = +20000$	
		${}^{\circ}G^{\mathrm{FeZr_3}}_{\mathrm{Zr:Fe}} - 3{}^{\circ}G^{\alpha\mathrm{Fe}}_{\mathrm{Fe}} - {}^{\circ}G^{\alpha\mathrm{Zr}}_{\mathrm{Zr}} = +20000$	
		${}^{\circ}G^{\mathrm{FeZr_3}}_{\mathrm{Fe:Zr}} - {}^{\circ}G^{\alpha\mathrm{Fe}}_{\mathrm{Fe}} - 3{}^{\circ}G^{\alpha\mathrm{Zr}}_{\mathrm{Zr}} = -73619.1094 + 21.6171610\ T$	
		${}^{\circ}G^{\mathrm{FeZr_3}}_{\mathrm{Zr:Zr}} - 4{}^{\circ}G^{\alpha\mathrm{Zr}}_{\mathrm{Zr}} = +20000$	
		${}^{0}L^{\mathrm{FeZr_3}}_{\mathrm{Fe,Zr:Fe}} = +5000$	
		${}^{0}L^{\mathrm{FeZr_3}}_{\mathrm{Fe,Zr:Zr}} = +5000$	
		${}^{0}L^{\mathrm{FeZr_3}}_{\mathrm{Fe:Fe,Zr}} = +80000$	
		${}^{0}L^{\mathrm{FeZr_3}}_{\mathrm{Zr:Fe,Zr}} = +80000$	
Fe-B	L	${}^{0}L^{\mathrm{L}}_{\mathrm{B,Fe}} = -140000 + 24.54T$	11)
		${}^{1}L^{\mathrm{L}}_{\mathrm{B,Fe}} = +5020$	
		${}^{2}L^{\mathrm{L}}_{\mathrm{B,Fe}} = +34444$	
	(αFe)	${}^{0}L^{(\alpha\mathrm{Fe})}_{\mathrm{B,Fe}} = -79000 + 30T$	
	((δFe))	${}^{1}L^{(\alpha\mathrm{Fe})}_{\mathrm{B,Fe}} = -37000$	
	(γFe)	${}^{0}L^{(\gamma\mathrm{Fe})}_{\mathrm{B,Fe}} = -48000 + 24T$	
		${}^{1}L^{(\gamma\mathrm{Fe})}_{\mathrm{B,Fe}} = -23000$	
	Fe_2B	${}^{\circ}G^{\mathrm{Fe_2B}}_{\mathrm{Fe:B}} - {}^{\circ}G^{\beta\mathrm{B}}_{\mathrm{B}} - 2{}^{\circ}G^{\alpha\mathrm{Fe}}_{\mathrm{Fe}} = -86940 + 7.41T$	
		$Tc^{\mathrm{Fe_2B}}_{\mathrm{Fe:B}} = +1018,\ \beta^{\mathrm{Fe_2B}}_{\mathrm{Fe:B}} = +1.91$	
	FeB	${}^{\circ}G^{\mathrm{FeB}}_{\mathrm{Fe:B}} - {}^{\circ}G^{\beta\mathrm{B}}_{\mathrm{B}} - {}^{\circ}G^{\alpha\mathrm{Fe}}_{\mathrm{Fe}} = -73418 + 6.5T$	
		$Tc^{\mathrm{FeB}}_{\mathrm{Fe:B}} = +600,\ \beta^{\mathrm{FeB}}_{\mathrm{Fe:B}} = +1.03$	
Zr-B	L	${}^{0}L^{\mathrm{L}}_{\mathrm{B,Zr}} = -230000 + 17.1T$	Present work
		${}^{1}L^{\mathrm{L}}_{\mathrm{B,Zr}} = -81000$	
		${}^{2}L^{\mathrm{L}}_{\mathrm{B,Zr}} = +10000$	
	(βZr)	${}^{0}L^{(\beta\mathrm{Zr})}_{\mathrm{B,Zr}} = -96000$	
	ZrB	${}^{\circ}G^{\mathrm{ZrB}}_{\mathrm{Zr:B}} - {}^{\circ}G^{\beta\mathrm{B}}_{\mathrm{B}} - {}^{\circ}G^{\alpha\mathrm{Zr}}_{\mathrm{Zr}} = -142600 - 67.38T + 8.8T\ln T$	
	ZrB_2	${}^{\circ}G^{\mathrm{ZrB_2}}_{\mathrm{Va:B}} - 2{}^{\circ}G^{\beta\mathrm{B}}_{\mathrm{B}} = +148600$	
		${}^{\circ}G^{\mathrm{ZrB_2}}_{\mathrm{Zr:Va}} - {}^{\circ}G^{\alpha\mathrm{Zr}}_{\mathrm{Zr}} = +34700$	
		${}^{\circ}G^{\mathrm{ZrB_2}}_{\mathrm{Va:Va}} = +60000$	
		${}^{\circ}G^{\mathrm{ZrB_2}}_{\mathrm{Zr:B}} - 2{}^{\circ}G^{\beta\mathrm{B}}_{\mathrm{B}} - {}^{\circ}G^{\alpha\mathrm{Zr}}_{\mathrm{Zr}} = -300900 - 12T + 1.5T\ln T + 0.00405T^2$	
		${}^{0}L^{\mathrm{ZrB_2}}_{\mathrm{Zr:B,Va}} = +660000$	
		${}^{1}L^{\mathrm{ZrB_2}}_{\mathrm{Zr:B,Va}} = -390000$	
	ZrB_{12}	${}^{\circ}G^{\mathrm{ZrB_{12}}}_{\mathrm{Zr:B}} - 12{}^{\circ}G^{\beta\mathrm{B}}_{\mathrm{B}} - {}^{\circ}G^{\alpha\mathrm{Zr}}_{\mathrm{Zr}} = -312130 + 516.1T - 66.3T\ln T$	
Fe-Zr-B	L	${}^{1}L^{\mathrm{L}}_{\mathrm{B,Fe,Zr}} = -130000$	Present work
	MB	${}^{1}L^{\mathrm{MB}}_{\mathrm{Fe,Zr:B}} = +158000$	

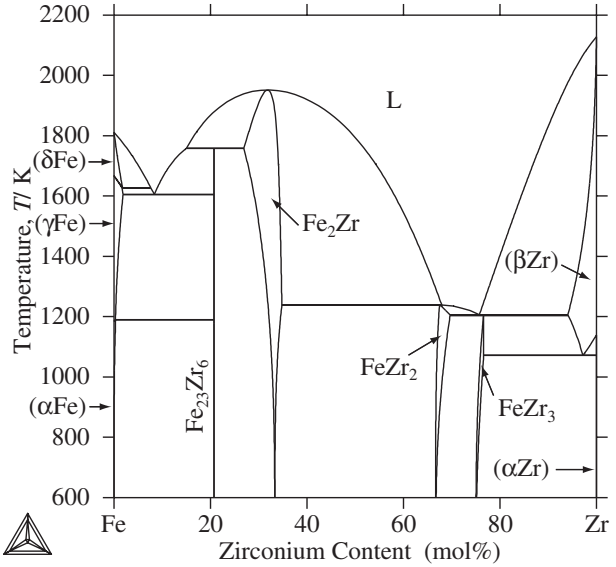

Fig. 1 The calculated Fe-Zr binary phase diagram.[19)]

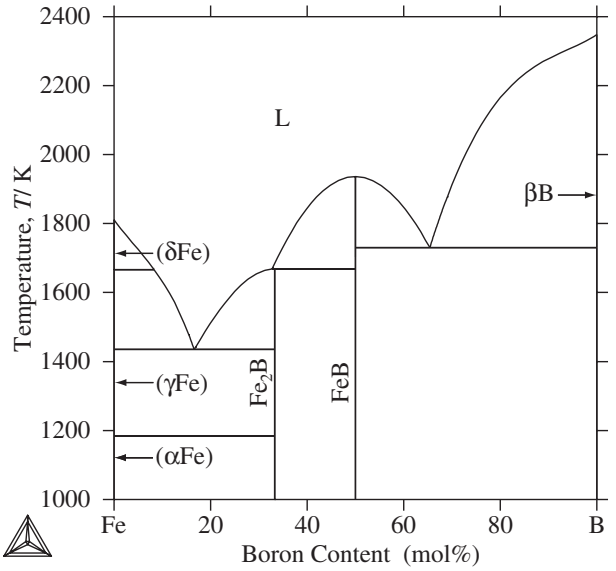

Fig. 2 The calculated Fe-B binary phase diagram.[11)]

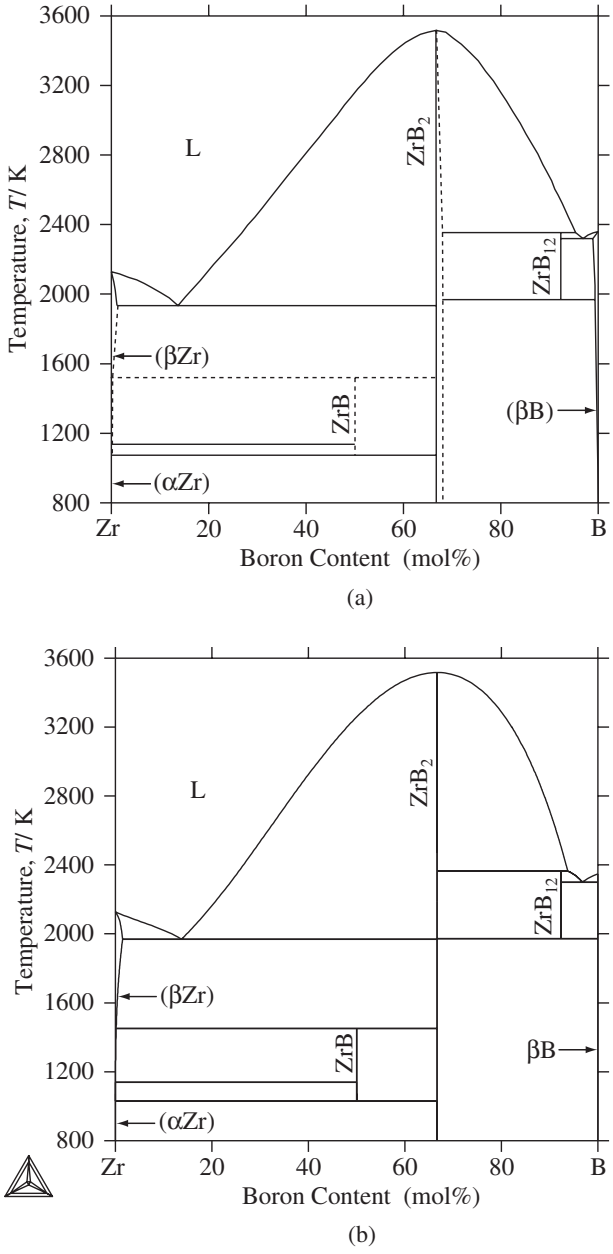

Fig. 3 (a) Assessed[28)] and (b) calculated Zr-B binary phase diagrams.

diagram indicates that the Zr-B system is composed of: a liquid (L), hcp ((αZr)), bcc ((βZr)), rhombohedral ((βB)), ZrB, ZrB_2, and ZrB_{12}. According to the experimental results, ZrB has a NaCl-type cubic structure,[29,30,32)] and its thermal stability is in the temperature range 1073–1523 K.[29)] Regarding ZrB_2 with an AlB_2-type hexagonal structure, the congruent melting temperature has been reported to be either 3313 K[29)] or 3523 K,[34)] and its homogeneity range is < 1 mol%.[31,34,35)] ZrB_{12} with an UB_{12}-type cubic structure was formed by the peritectic reaction at $T = 2303$ K.[34)] The eutectoidal decomposition of this phase was reported to be around 1983 K.[31)] The solubility of boron in both αZr and βZr appears to be < 1 mol%.[31)] Concerning the thermodynamic properties of this binary system, both the enthalpy of formation[37–39)] and the heat capacity[40)] of ZrB_2 are available in the literature. Thermodynamic assessment of this binary system has been carried out by Rogl and Potter,[41)] where the allotropic transformation of Zr and the formation of ZrB were not taken into account.

In this study, the thermodynamic parameters were re-evaluated using the formation enthalpies of the borides obtained from our first-principles calculations, as well as available experimental data. It was assumed that Zr was insoluble in rhombohedral βB because of its negligible solubility.

The enthalpy of formation data of the borides obtained from our first-principles calculations is listed in Table 2. Although the stable state of pure B was taken as being rhombohedral βB in the SGTE data,[9)] each value listed in Table 2 is referred to as hcp αZr and rhombohedral αB. As discussed in a previous paper,[11)] we regarded the calculated values relative to αZr and αB as being the formation enthalpy relative to αZr and βB because of the small difference in phase stability between αB and βB (17.4 meV/atom

Table 2 The calculated enthalpy of formation of various borides in the Zr-B system.

Phase	Space group	This study		Experimental
		First-principles	Thermodynamic analysis	
ZrB(NaCl-type)	$Fm\bar{3}m$	−39.6	—	—
ZrB(FeB-type)	*Pnma*	−67.1	−72.6	−79.3*[41]
ZrB_2	*P6/mmm*	−100.3	−100.6	-107.7 ± 1.7[37]
				-108.9 ± 2.1[38]
				−93[39]
ZrB_{12}	$Fm\bar{3}m$	−24.1	−22.5	—

*Estimated value

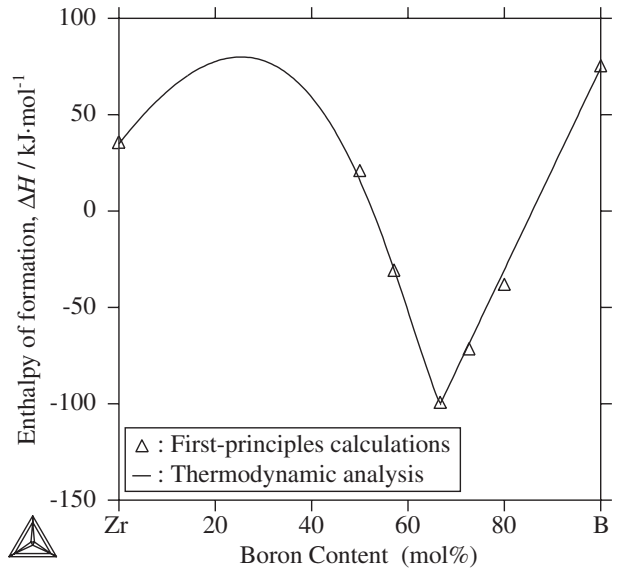

Fig. 4 Variation in the enthalpy of formation of ZrB_2 with composition.

(1.68 kJ/mol[42]) compared with the formation enthalpies of the borides. According to the results, the calculated enthalpy of formation of ZrB_2 is in good agreement with the experimental values.[37–39] For ZrB, although this boride has been reported to have a NaCl-type cubic structure, our first-principles calculations showed that ZrB with an FeB-type structure was energetically more stable than the NaCl-type ZrB, where the total energy of the FeB-type ZrB was calculated using information on the atomic positions for an FeB-type TiB. Thus, we adopted the calculated enthalpy of formation for the FeB-type ZrB in this analysis. It is noteworthy that although there is no experimental information on the formation of the FeB-type ZrB, an FeB-type monoboride forms in both the Ti-B and the Hf-B binary systems. Furthermore, the calculated enthalpy of formation of the FeB-type ZrB was close to the estimated value (−79.3 kJ/mol[41]) using information on the experimental isothermal section diagram of the Hf-Zr-B system[43] and the description of the Gibbs energy of HfB.[44] The evaluated thermodynamic parameters are listed in Table 2. The calculated results reproduce the experimental phase diagram nicely, along with the enthalpy of formation obtained from our first-principles calculations, as shown in Fig. 3 and Table 2, respectively. Figure 4 shows the variation in the enthalpy of formation of ZrB_2 with composition. The symbols denote the values obtained from a ground state analysis on this boride by constructing superstructures derived from an AlB_2-type structure, following the same procedures as described in a previous paper.[11] The solid line denotes the results evaluated by fitting the thermodynamic parameters corresponding to the excess enthalpy terms in eq. (8) to the formation enthalpy obtained from the first-principles calculations. The calculations indicate that the phase stability of this boride substantially decreases as the composition deviates from the stoichiometric point, resulting in a steep change in the enthalpy of formation of ZrB_2 around the stoichiometric point. This may be responsible for the limited homogeneity range of < 1 mol%. It is noteworthy that according to a previous result,[11] the change in the enthalpy of formation of NbB_2 with the same structure as that of ZrB_2 around the stoichiometric point was gradual, in contrast to the case of ZrB_2, and this may correspond to this boride exhibiting a homogeneity range of about 5 mol%.[15]

3.4 The Fe-Zr-B ternary system

In the Fe-Zr-B ternary system, the isothermal section diagram at $T = 1123$ K has been reported over the entire composition range,[45] and the phase boundaries at the Fe-ZrB_2 section have been investigated using thermal analysis.[46] According to the experimental results, there is no information on the ternary compound in this ternary system. The binary borides, except for FeB and ZrB, were treated as being pure binary phases because of the negligible solubility of a third element. In this modelling, the crystal structure of ZrB was assumed to be an FeB-type structure, following our results obtained from first-principles calculations, as already mentioned in Section 3.3, and thus, the Gibbs energies of FeB and ZrB were described by a single expression using the two-sublattice model with the formula $(Fe,Zr)_1B_1$ (which are hereafter denoted as the MB phase). The ternary thermodynamic parameters were evaluated in such a way that the calculated phase diagrams would reproduce the experimental phase boundaries,[45,46] and the evaluated parameters are listed in Table 1. The calculated isothermal section diagram at $T = 1123$ K is shown in Fig. 5, together with the experimental phase diagram.[45] Although there are no experimental data available, a low solubility of Fe in ZrB was introduced to obtain the phase equilibria between ZrB and Fe_2Zr. The calculated results are in agreement with the experimental phase equilibria, except for the absence of those relevant to $FeZr_3$ in Fig. 5(b), which has been included in the assessed Fe-Zr phase diagrams.[16,17] Figure 6 shows the calculated vertical section diagram along

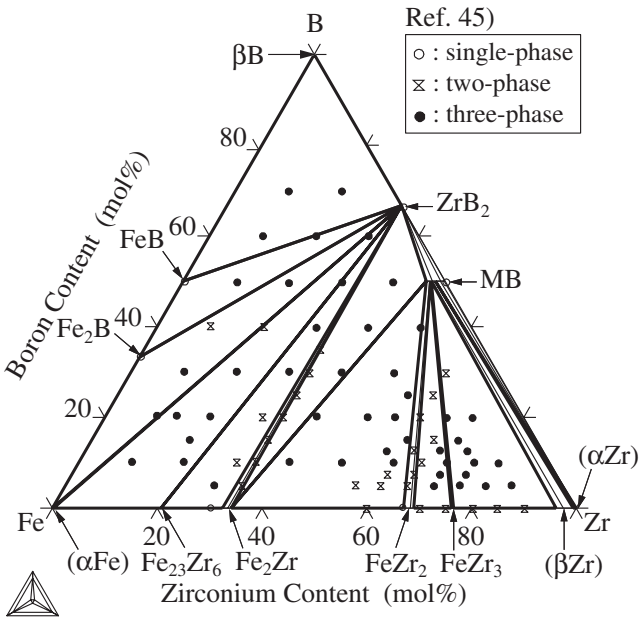

(a)

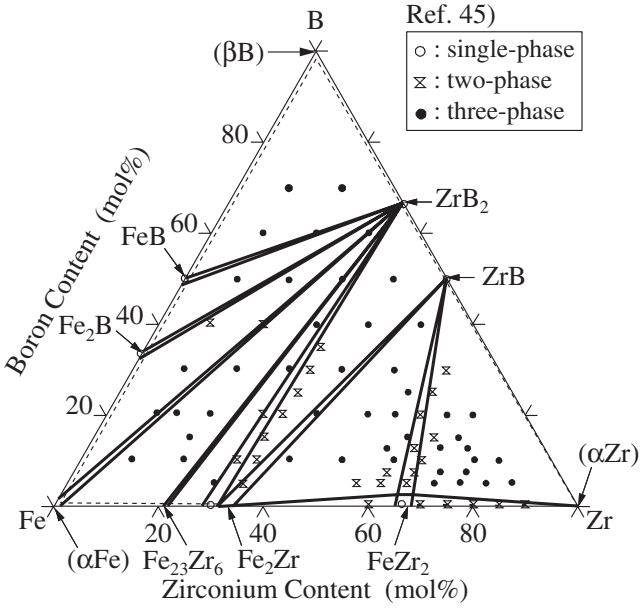

(b)

Fig. 5 (a) Calculated and (b) experimental[45] isothermal section diagrams of the Fe-Zr-B ternary system at 1123 K.

the Fe-ZrB_2 join, for comparison with the experimental data determined using thermal analysis.[46] The calculated results are consistent with the experimental data.

4. Conclusions

A thermodynamic analysis of the Fe-Zr-B ternary system has been carried out using the CALPHAD method, mainly based on available experimental data. Among the three binary systems relevant to this ternary phase diagram, the thermodynamic descriptions of the Fe-Zr and Fe-B binary systems were taken from previous studies. For the Zr-B binary system, the thermodynamic parameters were evaluated by incorporating thermodynamic properties of the

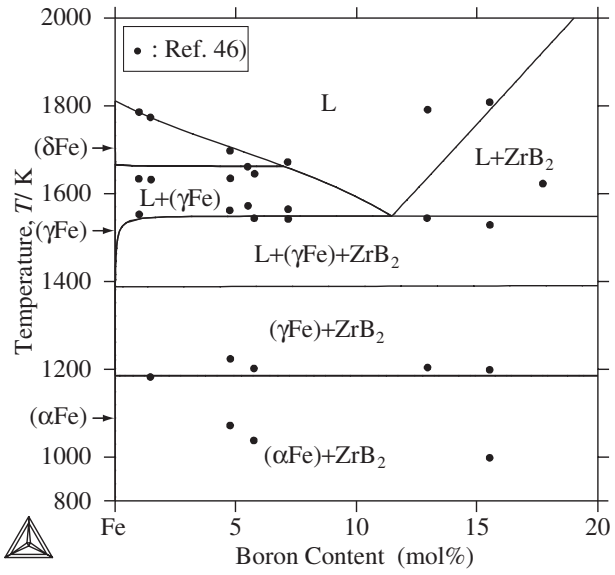

Fig. 6 The calculated vertical section diagram along the Fe-ZrB_2 join.

borides into the CALPHAD approach. The results obtained are summarized as follows:

(1) Our first-principles calculations showed that ZrB with an FeB-type structure was energetically more stable than that with a NaCl-type structure.
(2) The thermodynamic parameters of the Zr-B binary system enabled us to obtain reproducible calculations of the formation enthalpies obtained from our first-principles calculations, as well as the experimental data on phase boundaries.
(3) The calculated Fe-Zr-B ternary phase diagrams agree well with the available experimental results.

Acknowledgement

The authors acknowledge financial support from Core Research for Evolutional Science and Technology (CREST), Japan Science and Technology Agency.

REFERENCES

1) K. Suzuki, N. Kataoka, A. Inoue, A. Makino and T. Masumoto: Mater. Trans. JIM **31** (1990) 743–746.
2) K. Suzuki, A. Makino, N. Kataoka, A. Inoue and T. Masumoto: Mater. Trans. JIM **32** (1991) 93–102.
3) K. Suzuki, M. Kikuchi, A. Makino, A. Inoue and T. Masumoto: Mater. Trans. JIM **32** (1991) 961–968.
4) K. Suzuki, A. Makino, A. Inoue and T. Masumoto: J. Appl. Phys. **74** (1993) 3316–3322.
5) *e.g.*, Y. Zhang, K. Hono, A. Inoue, A. Makino and T. Sakurai: Acta Mater. **44** (1996) 1497–1510.
6) P. Blaha, K. Schwarz, G. K. H. Madsen, D. Kvasnicka and J. Luitz: *WIEN2k, An Augmented Plane Wave Plus Local Orbitals Program for Calculating Crystal Properties*, (Techn. Universität Wien, Austria, 2002) ISBN 3-9501031-1-2.
7) J. P. Perdew, K. Burke and Y. Wang: Phys. Rev. B **54** (1996) 16533–16539.
8) P. Villars: *Pearson's Handbook, Crystallographic Data for Intermetallic Phases, Desk Edition*, (ASM International, Materials Park, Ohio, USA, 1997).
9) A. T. Dinsdale: Calphad **15** (1991) 317–425.
10) O. Redlich and A. T. Kister: Ind. Eng. Chem. **40** (1948) 345–348.

11) K. Yoshitomi, Y. Nakama, H. Ohtani and M. Hasebe: ISIJ Int. **48** (2008) 835–844.
12) G. Inden: Proc. CALPHAD V, Düsseldorf, 1976, III-(4)-1.
13) M. Hillert and M. Jarl: Calphad **2** (1978) 227–238.
14) M. Hillert and L.-I. Staffansson: Acta Chem. Scand. **24** (1970) 3618–3626.
15) C. A. Nunes, D. Kaczorowski, P. Rogl, M. R. Baldissera, P. A. Suzuki, G. C. Coelho, A. Grytsiv, G. André, F. Boureé and S. Okada: Acta Mater. **53** (2005) 3679–3687.
16) H. Okamoto: J. Phase Equilib. **18** (1997) 316.
17) H. Okamoto: J. Phase Equilib. Diffusion **27** (2006) 543–544.
18) F. Stein, G. Sauthoff and M. Palm: J. Phase Equilib. **23** (2002) 480–494.
19) M. Jiang, K. Oikawa, T. Ikeshoji, L. Wulff and K. Ishida: J. Phase Equilib. **22** (2001) 406–417.
20) P. K. Liao and K. E. Spear: *Phase Diagrams of Binary Iron Alloys*, ed. by H. Okamoto (ASM International Metals Park, OH, USA, 1993) pp. 41–47.
21) T. G. Chart: Comm. Comm. Eur., 7210-CA/3/303 (1981).
22) L. Kaufman, B. Uhrenius, D. Birnie and K. Taylor: Calphad **8** (1984) 25–66.
23) H. Ohtani, M. Hasebe, K. Ishida and T. Nishizawa: Trans. Iron Steel Inst. Jpn. **28** (1988) 1043–1050.
24) L.-M. Pan: In B. Sundman, ed., Scientific Group Thermodata Europe (SGTE) Solution Database Ver.2, Division of Computational Thermodynamics, (Royal Institute of Technology, Stockholm, Sweden, 1994).
25) B. Hallemans, P. Wollants and J. R. Roos: Z. Metallkd. **85** (1994) 676–682.
26) M. Palumbo, G. Cacciamani, E. Bosco and M. Baricco: Calphad **25** (2001) 625–637.
27) T. Van Rompaey, K. C. Hari Kumar and P. Wollants: J. Alloy. Compd. **334** (2002) 173–181.
28) H. Okamoto: J. Phase Equilib. **14** (1993) 261–262.
29) F. W. Glazer and B. Post: Trans. AIME **197** (1953) 1117–1118.
30) H. Nowotny, E. Rudy and F. Benesovsky: Monatsh. Chem. **91** (1960) 963–974.
31) E. Rudy: *Ternary Phase Equilibria in Transition Metal-Boron-Carbon-Silicon Systems, Part V*, (Air Force Materials Laboratory, Air Force Systems Command, Wright-Patterson Air Force Base, OH, USA, 1960) p. 689.
32) O. I. Shulishova and I. A. Shcherbak: Inorg. Mater. **3** (1967) 1304–1306.
33) J. S. Haggerty, J. L. O'Brien and J. F. Wenckus: J. Cryst. Growth **3/4** (1968) 291–294.
34) K. I. Portnoi, V. M. Romashov and L. N. Burobina: Sov. Powder Metall. Met. Ceram. **9** (1970) 577–580.
35) K. I. Portnoi and V. M. Romashov: Sov. Powder Metall. Met. Ceram. **11** (1972) 378–384.
36) Y. Champion and S. Hagège: J. Mater. Sci. Lett. **11** (1992) 290–293.
37) E. J. Huber, E. L. Head and C. E. Holley: J. Phys. Chem. **68** (1964) 3040–3042.
38) G. K. Johnson, E. Greenberg, J. L. Margrave and W. N. Hubbard: J. Chem. Eng. Data **12** (1967) 137–141.
39) E. P. Kirpichev, Yu. I. Rubtsov, T. V. Sorokina and V. K. Prokudina: Russ. J. Phys. Chem. **53** (1979) 1128–1130.
40) R. H. Valentine, T. F. Jambois and J. L. Margrave: J. Chem. Eng. Data **9** (1964) 182–184.
41) P. Rogl and P. E. Potter: Calphad **12** (1988) 191–204.
42) S. Shang, Y. Wang, R. Arroyave and Z.-K. Liu: Phys. Rev. B **75** (2007) 092101-1–092101-4.
43) D. P. Harmon: Techn. Rept. No. AFML-TR-65-2, Part II, Vol. VI, (Wright Patterson Air Force Base, OH, USA, 1966) pp. 1–64.
44) P. Rogl and P. E. Potter: Calphad **12** (1988) 207–218.
45) Yu. B. Kuz'ma, V. I. Lakh, Yu. V. Voroshilov, B. I. Stadnyk and V. Ya. Markov: Russ. Metall. **6** (1965) 88–90.
46) A. K. Shurin and V. E. Panarin: Russ. Metall. **5** (1974) 192–195.